European Rotorcraft Forum

EXPERIMENTAL EVALUATION OF THE AERODYNAMIC ROTOR/PROPELLER INTERACTIONS IN HYBRID COMPOUND HELICOPTERS

Lauriane Lefevre, Jérôme Delva, Vianney Nowinski - ONERA (France)
Univ. Lille, CNRS, ONERA, Arts et Métiers Institute of Technology, Centrale Lille, UMR 9014-LMFL-Laboratoire de Mécanique des Fluides de Lille - Kampé de Fériet, F-59000, Lille, France.

Corresponding author e-mail: lauriane.lefevre@onera.fr

Abstract
This paper focuses on the experimental evaluation of the rotor/propeller interactions in hybrid compound configurations. Experiments were conducted in the ONERA L2 large size-low speed wind tunnel with a 1/7.7 Dauphin 365N model and a four-bladed small-scale propeller. The exhaustive characterization of the propeller's performance was previously realized. Measurements were conducted using two six-component scales, accelerometers, and toppers to monitor the rotational speeds. Different flight conditions were set with variating wind speed, propeller rotational speed, and propeller position. Comparing the isolated characterizations of the rotor and the propeller with the complete assembly highlighted the influence of the interactions on the performances of the rotating elements. Variating the location of the propeller around the helicopter allowed the determination of the optimal position to maximize the performance.

NOTATION

V	Free stream velocity (m/s)
V_{tip}	Blade tip rotation velocity (m/s)
μ	Advance ratio ($\mu = {V}/{V_{tip}}$)
R	Rotor radius
Ω	Rotational velocity (rpm)
b	Number of blades of the rotor
c	Blade chord (m)
σ	Rotor solidity ($\sigma = \frac{b\,c}{\pi\,R}$)
S	Rotor disk surface (m²)
ρ	Air density (kg/m^3)
Fz	Thrust (N)
Z_{bar}	Thrust coefficient ($\bar{Z} = \frac{100.Fz}{\frac{1}{2}\rho S\sigma(R\Omega)^2}$)

1. INTRODUCTION

Helicopters have always been recognized for their hovering and vertical take-off and landing (VTOL) capabilities. While the demand has increased due to the multiplication of air transport, the military and civil needs cannot be reached by the classical configurations due to 1) a limited maximum speed, roughly around 300 km/h for conventional configurations, 2) a low load capacity, 3) a small autonomy, and 4) a questionable comfort due to vibrations and noises … In that context, the compound helicopters have been designed. Including additional rotors and/or lift wings, these setups entail a rotor slow-down allowing the device to reach higher speeds without encountering compressibility issues. This study focuses on the hybrid compound helicopter, equipped with two side propellers mounted on a lift-wing. Two examples are the Eurocopter X3 (Figure 1) that reached the velocity of 472 km/h in 2014, and the Airbus Helicopters RACER (Figure 2) that is expected to have a cruise speed of 400km/h. On top of increasing the maximum cruise speed, the side propellers create an efficient anti-torque while preserving hovering abilities.

Figure 1 - Eurocopter X3

Figure 2 - Airbus Helicopters RACER

Presented at 47th European Rotorcraft Forum, United Kingdom, 7-9th September, 2021

However, compound helicopters are subject to complex and important interactions due to the multiplication of rotating elements. Numerical researches have been conducted to study rotor/wing [1]–[5], rotor/fuselage [6]–[8], wing/propeller [9], and rotor/propeller interactions [10], but very few experimental investigations are available to date. In this context, this paper presents the experimental study of aerodynamic rotor/propeller interactions by analyzing the resulting loads of the rotors depending on the configuration.

Experiments took place in the ONERA L2 large size-low speed wind tunnel with a 1/7.7 scale DAUPHIN 365N model and a small-scale propeller. The components were chosen to mimic the Eurocopter X3 configuration. Varying wind speed, rotational speed, and propeller position, the ideal flight conditions were identified.

2. EXPERIMENTAL SETUP

2.1. The Main Rotor

A 1/7.7 scale DAUPHIN 365N model made of glass fiber was used for this study (Figure 2). This test rig has been widely studied at ONERA [11], [12]. The length of the helicopter is 1.467 meters and its height is 0.417 meters. The rotor is fully articulated and equipped with four rectangular blades with the following characteristics: profile 0A209, a chord of 0.05 m, linear torsion angle of -16 °/m. The blades are made of glass-filled nylon and are geometrically similar to the full-scale helicopter. The rotor diameter is 1.5 meters and is tilted 4° towards the nose of the device.

The blade tip Mach is not maintained compared to the full-scale helicopter, but the thrust coefficient is preserved ($Z_{bar} = 14.5$ to mimic a medium flight condition). The nominal rotational speed is 1272 rpm, which corresponds to a blade tip speed of 100 m/s. The advancing side of the rotor is to starboard.

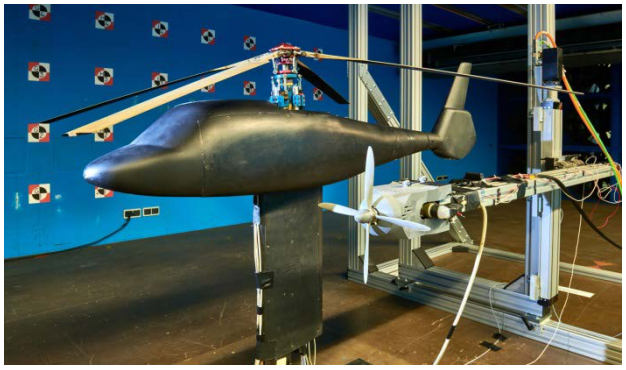

Figure 3 - Installation of the small-scale Dauphin 365N and APC11x06-4 propeller

The mechanical assembly is composed of

- A rotor mast that is geometrically similar to the spheriflex of the SA365 including a hollow shaft, a four-bladed hub, and a swashplate piloted by 3 electric jacks associated with a pitch copying system;

- A motor-reduction unit composed of a variable frequency motor FV76 providing a power of 4 kW for a maximum rotational speed of 1400 rpm, and a gearbox with a freewheel;

- A connecting plate between the support mast, the motorization, the rotor mast, and the fuselage of the device;

- A set of instrumentation composed of a 12-track rotating collector, 2 magnetic topping sensors, a PT100 platinum probe to measure the engine temperature, and a potentiometric track to measure the model's incidence.

The loads are measured using a 6-axis aerodynamic balance, and accelerometers are set in two directions. The collective and cyclic pitch angles are controllable and measurable to mimic real flight scenarios. The blade yaw and drag angles are also measured.

An air-cooling circuit is implemented to limit the motor heating during the campaign. The pressure is set at 2 bars. The loads created by the cooling system are considered negligible. The measurements offset is corrected to encounter the influence of the pressure.

For each test, the data is measured for 30 seconds at a frequency of 3000 Hz. Measurements are recorded and monitored with LabVIEW, also used to set the rotational speeds of the rotating elements. The post-treatment is performed using a house-made python code. The study is conducted in standard atmospheric conditions. The variation of ambient temperature, pressure, and humidity are registered. No correction to the wind speed is applied since the maximal air density variation observed during the campaign is less than 2%.

2.2. The Side Propeller

2.2.1 Equipment

The first step of this experimental study consisted of characterizing the isolated propeller for different flight scenarios. The propellers were chosen to mimic the Eurocopter X3 diameter, thrust, and tip speed.

A 4-blade off-the-shelf propeller supplied by APC Propeller was used. To preserve the geometric ratio between the main rotor and the propeller, the diameter is 0.28 meters (11 inches). The blade

torsion angle is 9°. The blades are made of glass-filled nylon. The geometry of the blade was provided by the supplier, and the 2D airfoil tables were obtained using the ONERA elsA RANS CFD software.

Measures are performed using the AMTI MC3A 6-axis balance. The characteristics are a non-linearity of ± 0.2 % at full scale and a transverse sensibility lower than 2%. The balance is connected to a GEN5 conditioner. The assembly is also equipped with a resistance thermometer (PT100). A linear temperature correction is applied to correct the divergence of the forces measured by the balance. The coefficients were determined experimentally in different conditions, and the correction was proven efficient.

2.2.2 Preliminary study

The exhaustive characterization of the propeller's performances in different flight conditions [13] allowed the measurement of the loads on the isolated propeller, and the comparison of the results without the influence of the rotor wake. The study of the effect of the side-slip angle on the performances proved that the wall and blockage effects are negligible considering the small dimensions of the propeller. The absence of stall for all flight conditions was also outlined.

To maximize the aerodynamic efficiency of the propeller, a tip cone has been set. A fairing has also been designed to isolate the aerodynamic loads from the flow created by the propeller wake and the wind. This preliminary study proved the efficiency of these devices.

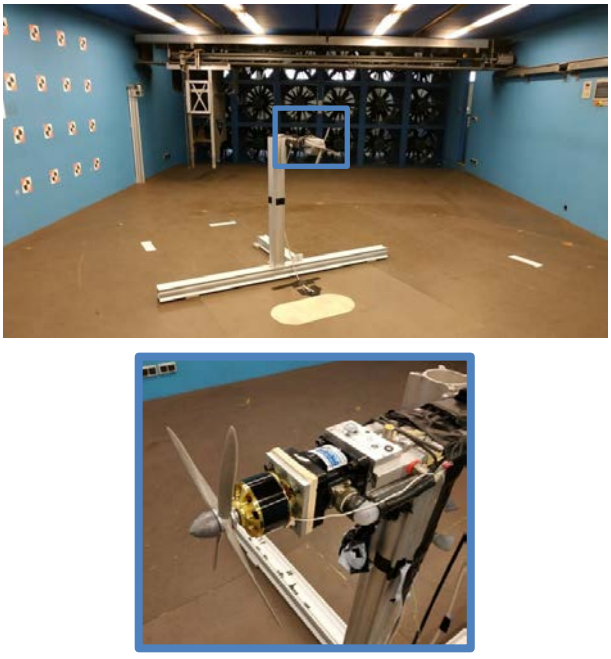

Figure 4 - Isolated small-scale propeller mounted in the L2 subsonic wind tunnel

Studying the side-slip angle also allowed the measurement of the direct effect of the rotor wake in hover. The results of the isolated propeller and the full mounting will be compared in this paper.

2.2.3 Numerical approach

This preliminary work validated the PUMA (Potential Unsteady Methods for Aerodynamics) code used at ONERA. Particularly used in the pre-design phases for fixed and rotating wings, this free wake code is based on a coupling between the kinematic and the free aerodynamic modules.

A rigid body assumption is used to build the kinematic module. The structure is composed of links and articulations, and the hypothesis of a negligible deformation regardless of the external constraints is made to simplify the computation. The aerodynamic module is determined using a free wake model and a lifting line approach.

The computation parameters were based on previous studies. Depending on the case, the last 3 to 5 wake revolutions were averaged and 8 to 15 revolutions were computed. While most of the cases reached convergence with these parameters, for low advance ratio or specific side-slip angles unsteadiness was important. Some numerical parameters had to be modified to stabilize the computation, which might have affected the obtained results.

The free wake approach presents several limitations: 1) only incompressible wakes are considered and 2) the theory is particularly adapted for tapered wings. Considering the very low speeds involved and the geometry of the blades, the up-listed limitations do not interfere with our case.

During the preliminary test campaign, a difference of 10-15% appeared between the numerical and the experimental results. When introducing an important side-slip angle, this divergence reached up to 30% for specific cases. However, considering the calculus hypothesis used in PUMA, the measurement uncertainties, and the very intrusive measurement bench that was not simulated, this approach validated the consistency of PUMA for simple test cases.

2.3. L2 wind tunnel

Experimental studies were conducted in the ONERA large size-low speed L2 wind tunnel. This installation has been in operation since 1968 for naval, industrial, and aeronautical applications with a large panel of measurement techniques.

The test section is 6 meters wide, 2.4 meters high, and 13 meters long. To adjust the assembly, a rotating plate with a diameter of 5.96 meters is

integrated into the wind tunnel floor. The measured drift angle is set with an over-estimated uncertainty of 0.1°. The center of the rotating disk is located 6.5 meters downstream of the honeycomb.

Downstream of the test section, a small divergence to a width of 2.8 meters is observed to fit 18 fans divided into 3 horizontal lines and 6 columns. All together, the fans provide a power of 125 kW, allowing the velocity to reach 19 m/s. The flow is then vented to the rear part of the hall where it freely diffuses to the sides and top before returning to the entrance of the tunnel with a low velocity.

The wind tunnel operates at ambient atmospheric conditions. The humidity, the ambient static pressure, and temperature are measured in the undisturbed air in the hall to evaluate the influence of the atmospheric conditions on the air density. No cooling devices are used to keep the flow at a constant low temperature but, considering the low velocities involved, the natural heat conduction only generates a 5°C per hour temperature increase in continuous operations at full power. The flow passage ensures the cooling of the electric engines of the fans.

The turbulence profile shows values up to 7.6% close to the walls, but less than 3% in the middle of the section. These values depend on the wind speed and the geometry of the tested bench.

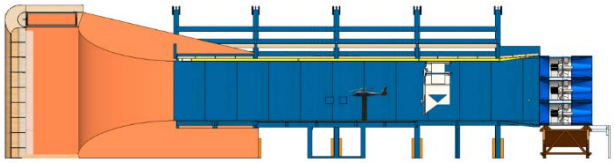

Figure 5 - Scheme of the INTROH bench mounted in the L2 subsonic wind tunnel

3. RESULTS

A parametric study was conducted considering different parameters:

- The wind speed varies from 0m/s to 19m/s, operating through all the L2 capabilities. Considering the nominal rotational speed of the rotor, the equivalent advance ratio can be calculated with μ = V/100. To suppress the inertial effects, a stabilization time is observed for each wind speed change.
- The rotational speed of the propeller varies from 0 rpm to 9000 rpm. The rotational speed is manually set with an uncertainty of ±30 rpm. The measurement uncertainty is less than 1%.
- The position of the propeller is modified in all three directions.

Considering the experimental constraints, the rotational speed of the helicopter is set at 1100±10 rpm for all the tests. The measurement uncertainty is less than 50rpm at the nominal rotational speed. The rotor thrust (Fz_rotor) is set at 99.3 ± 3 N, which corresponds to a thrust coefficient $\bar{z} = 14.5$. The longitudinal load (Fx_rotor) is set to counterbalance the drag created by the isolated fuselage [±0.5N]. The longitudinal flap angle (β_{1s}) is zero [±0.5°]. In all the following figures, the 95% confidence interval is plotted in red.

The propeller is placed on the advancing side of the rotor. The nominal position has been determined using the Eurocopter X3 dimensions: 0.14m ahead of the rotor center (one propeller radius), 0.375m away from the fuselage (half a rotor radius), and 0.28m below the rotor head. The positions will be referred to using the following referential: considering $\vec{x}$ from the nose to the tail of the propeller, +1X represents a translation of one propeller radius (0.14m) to the back of the helicopter. In this case, the propeller is aligned with the rotor head. When placed at +2X, the propeller is located 0.14m behind the rotor head. In position -1Y the propeller is moved away from the fuselage. The position -1/2Z allows the study of the interactions when the propeller is moved closer to the ground.

3.1. Influence of the Advance Ratio

Increasing the advance ratio decreases the thrust provided by the propeller (Figure 6). This observation is due to the modification of the local angle of attack of the flow on the propeller blades.

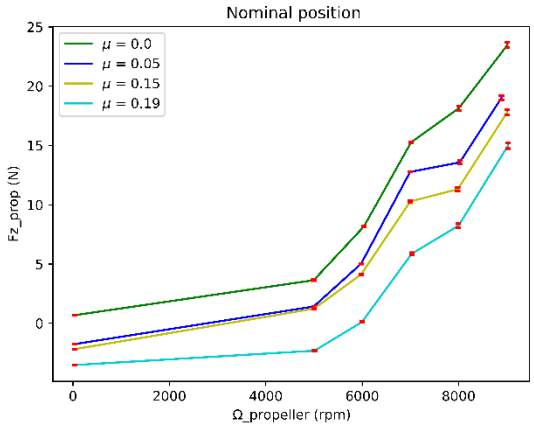

Figure 6 - Influence of the advance ratio on the thrust of the propeller in the nominal position

Indeed, for μ = 0.00, numerical studies [14] predict that the propeller is fully immersed in the rotor wake. The rotor wake creates the equivalent of a 14m/s flow impinging the propeller at 90°. In that case, an important increase of torque variations is

observed on the propeller, while the mean thrust remains unchanged.

The experimental characterization of the isolated propeller depending on the side-slip angle showed that the resulting thrust was increased with a 90° flow. When the propeller is not activated and without the influence of free-stream velocity, the thrust should be zero. This characteristic was not verified during the preliminary study (Figure 7), highlighting possible measurement uncertainties. It has been chosen not to correct the offset during the post-treatment. It can however be seen that the effects at 45° would be superior if the offset was compensated manually.

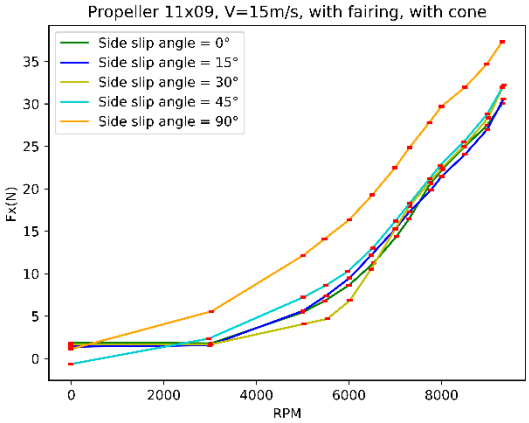

Figure 7 - Influence of the side-slip angle on the thrust of the isolated propeller

When increasing the advance ratio, the influence of the rotor wake on the propeller decreases. For μ ≥ 0.10, the numerical approach predicts that the rotor wake does not directly impinge the propeller. Both wakes are pushed towards the tail of the helicopter due to the influence of the freestream velocity. Only minor wake interactions are observed and lead to a small increase of the propeller thrust.

For the intermediary case (μ = 0.05), it is predicted that the propeller is only partially immersed in the rotor wake. In this configuration, a combination of both cases is observed, and a decrease of propeller torque and thrust appears. This numerical result is not entirely verified experimentally since the curves for μ = 0.05 and μ = 0.15 are similar for small rotational speeds.

The study of the isolated propeller (*Figure 8*) highlights the influence of the freestream velocity on the propeller. In conclusion, the presence of the rotor amplifies the influence of the advance ratio on the resulting thrust for low speeds.

On the other hand, the wind creates a force on the propeller's disk, as shown by the offset of the measures at Ωpropeller = 0 rpm. This force is negligible compared to the thrust at high rotational speeds. The curve without wind speed also shows a good initialization of the balance since the measured thrust is null when the propeller is inactive.

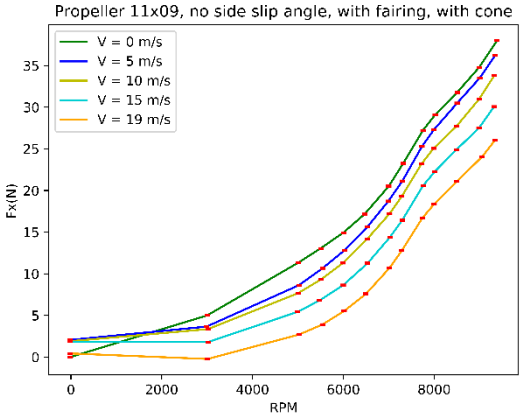

Figure 8 - Influence of the wind speed on the thrust of the isolated propeller

3.2. Influence on the Rotor

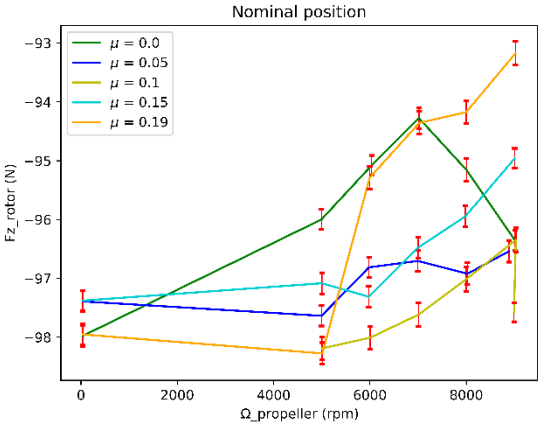

Figure 9 - Influence of the rotational speed of the propeller on the thrust of the rotor

A small influence of the propeller on the rotor has been measured (Figure 9). Sudden variations can be observed, for example for μ=0.0 and μ=0.19. These divergences are consequent to the adaptation of the rotor inlet power to maintain the nominal rotational speed despite the heating of the motor. These variations should not be considered for the analysis.

When increasing the rotational speed of the propeller, the thrust of the rotor decreases by 1% to 3%. On the other hand, the numerical approach predicts that the propeller/rotor interactions lead to a

gain of 2% of the rotor's thrust. In hover, depression is predicted on the rotor disk upstream of the propeller and is compensated by an overpressure zone caused by the propeller wake.

The difference in the results can be explained by the uncertainty of both approaches: in the experimental process measurement uncertainties arise, and the thrust is set manually by the operator with limited precision as shown by the offset of thrust when the propeller is not active. The numerical approach used for this study only considers the two rotors. While the influence of the fuselage has been proven to be small, it may slightly modify the interactional effects. Additionally, the influence of the propeller fairing and support bench is not considered in the numerical approach

While the 95% interval confidence is small for all the other curves due to the important number of points, the interval is much larger in this study. Considering the uncertainties listed above, it can be considered that the influence of the propeller on the rotor is negligible.

3.3. Influence of the Interactions in Hover

A good correlation is observed between the isolated propeller and the propeller in the nominal position at Ωpropeller = 0 rpm, thus proving the good initialization of the balance and the absence of rotor/propeller interactions in that case (Figure 10).

However, the propeller's thrust is up to 30% smaller compared to the isolated propeller. On the other hand, numerical studies predict an increase of 2% to 5% due to the rotor/propeller interactions. The comparison with the numerical approach made during the campaign with the isolated propeller showed a slight overestimation of the measures compared to the computed results. The difference can be explained by experimental and numerical uncertainties. Further tests will be conducted to identify the sources of difference between the two campaigns.

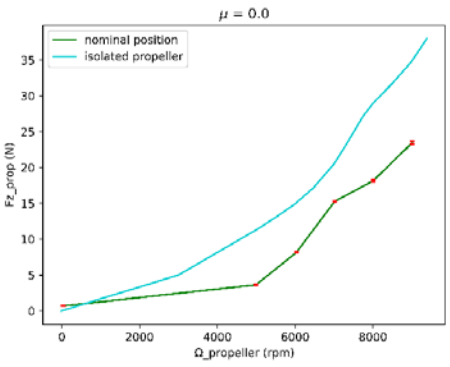

Figure 10 - Influence of the installation on the thrust of the propeller in hover

Performances of the propeller are maximized when the propeller is moved towards the tail of the device (position +2X, Figure 11). The thrust of the propeller is increased at the nominal rotational speed (Ωpropeller = 7656 rpm) and reaches the thrust measured on the isolated propeller. The performances for all other rotational velocities remain unchanged.

In the nominal configuration, the propeller is placed one propeller radius (0.14m) ahead of the rotor head, and it is moved 0.14m behind the rotor head in the +2X position. The influence of the rotor wake should be the same in both positions in hover. The peak of thrust observed at the nominal rotational speed might be the result of resonance effects. It can also be observed that the measured thrust when the propeller is inactive is not null. In this study, the propeller is situated under the advancing side of the rotor. It can be guessed that the small thrust measured is due to the influence of the rotation of the rotor blade on the development of the wake.

Further tests will be conducted on the retreating side of the rotor to study the asymmetry of the rotor wake in hover and its influence on the propeller. PIV measurements will also be conducted to verify the homogeneity of the rotor wake in hover. Due to measurement discrepancies, conclusions for the +1X position could not be drawn in hover.

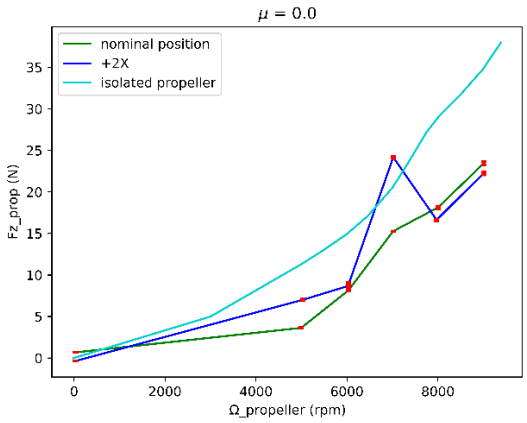

Figure 11 - Influence of the position of the propeller on the thrust in hover

Moving the propeller closer to the ground (-1/2Z) leads to a loss of thrust of 20% for all rotational speeds of the propeller (Figure 12). This observation is due to the limited influence of the rotor wake on the propeller in this configuration. While the propeller is still completely immerged in the rotor wake that is characterized by a constant speed over its entire height, the ground effects might not be negligible. In this case, the rotor wake velocity could be limited by the ground interactions.

The propeller could also be immerged in rotor wake recirculation, therefore modifying the local angle of attack of the flow on the blades. This first study highlights the positive influence of the rotor/propeller interactions in hover at nominal height.

The lateral displacement of the propeller (-1Y) does not influence the performance of the propeller. However, to limit the size of the structure, the nominal lateral position has to be preferred. The divergent point at Ωpropeller=0rpm should not be considered for the analysis. Repeatability tests will be conducted to validate the rest of the measures.

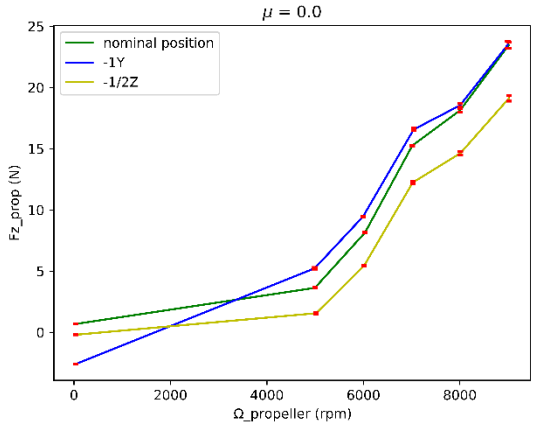

Figure 12 - Influence of the position of the propeller on the thrust in hover

3.4. Influence of the Interactions at High Speeds

The same conclusions as the one in hover can be made: when moving the propeller towards the tail of the helicopter, the thrust is increased at the nominal rotational speed (Figure 13). However, in the position +2X, the resulting thrust for all other rotational speeds is smaller than in the nominal position.

Preliminary studies predicted that no direct interaction between the rotor wake and the propeller for μ ≥ 0.10. However, this conclusion might not be verified for the +2X position. Therefore, it can be assumed that the influence of the rotor wake is stronger in this position, causing the small loss of thrust observed.

The study of the influence of the modification of the longitudinal position, therefore, showed that aligning the propeller with the rotor center (position +1X) is beneficial for the performance of the device at high speeds.

It can also be seen that, except for the nominal rotational speed, the thrust of the propeller is 30% smaller than the thrust measured on the isolated bench for all positions. This validates the conclusion drawn in hover, and the necessity to perform complementary tests.

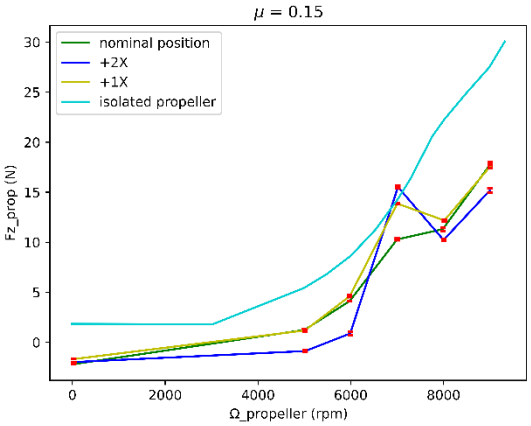

Figure 13 - Influence of the position of the propeller on the thrust at high speeds

At high speeds, the lateral displacement of the propeller does not impact the propeller's performance (Figure 14). However, moving the propeller closer to the ground leads to an increase of thrust at small rotational speeds. This shows a stronger influence of the wind on the propeller due to the absence of interaction between the propeller and the rotor wakes. This observation validates the conclusion made on the influence of the rotor wake on the thrust of the propeller (Figure 6).

At high rotational speeds, moving the propeller closer to the ground does not impact the resulting thrust. This observation validates the hypothesis of ground effects in hover in the position -1/2Z. The absence of direct rotor/propeller interactions in the nominal position at high advance ratios is also highlighted, as predicted by the numerical approach.

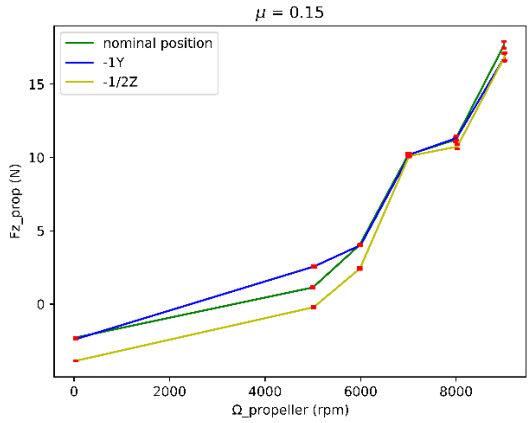

Figure 14 - Influence of the position of the propeller on the thrust at high speeds

The study of the influence of the propeller position on the performances of the device showed that the vertical and the transversal displacement of the propeller are not beneficial. It could however be seen that the performances are increased when the propeller is moved towards the tail of the helicopter. Further tests will be conducted to study the influence of the lateral and vertical displacement in the position +1X, previously identified as beneficial for the performances of the helicopter.

3.5. Discussion

During the campaign, an important divergence has been observed on the propeller's balance. Some test cases were not interpretable, and no repeatability analysis could be conducted. The presented results will be verified in further tests.

A temperature divergence on the propeller's balance has been identified in the preparatory phase. This divergence has been corrected with linear experimentally set parameters, and the correction has been proven to be efficient.

The analysis of the 95% confidence interval shows a good concordance of the measures.

During the tests, it has been observed that the power required to fly for all values of $\mu \geq 0.10$ remains constant. However, the required power is increased by 14% in hover and by 7% at $\mu=0.05$. This observation highlights the beneficial effect of the wind on the rotor. A similar observation was made on the propeller.

4. CONCLUSION

This study aimed to prove the efficiency of the hybrid compound helicopters and to quantify the influence of the rotor/propeller interactions on the efficiency of the device.

Increasing the advance ratio leads to a reduction of propeller thrust due to the modification of the angle of attack of the flow on the propeller. While the same observation was made for the isolated propeller, this characteristic is enhanced by the rotor/propeller interactions.

Reciprocally, the influence of the propeller on the rotor is negligible and cannot be determined with certainty considering the available tools. The ideal position is therefore determined using only the propeller's data.

Studying the influence of the position of the propeller on the performance of the device highlighted two conclusions: 1) moving the propeller towards the tail of the rotor increases its performance, and 2) moving the propeller away from the fuselage or closer to the ground is not beneficial. Regarding these results, the +1X position will be preferred for the rest of the study. In this position, the propeller is placed 0.375m away from the fuselage (y=-0.375m), 0.28m below the rotor head (z=-0.28m), and aligned with the rotor center (x=-0.0m).

PIV experiments will be conducted to determine the velocity field around the helicopter for the nominal and the +1X positions. This analysis will question the observations made above. The validity of the measures will be discussed, and the need to replace the propeller balance will be evaluated.

Further tests will be realized to validate the first conclusions and to explore other configurations. The influence of the transversal or vertical displacements in the +1X position will be studied. The propeller will also be installed on the retreating side of the helicopter to highlight the influence of the asymmetric rotor wake.

5. ACKNOWLEDGMENT

The authors gratefully acknowledge the financial support given by ONERA and the region Hauts-de-France. The technical support of Ronan Boisard and François Richez for the numerical study is thanked. Antoine Dazin is also thanked for his help throughout the test campaign.

6. REFERENCES

[1] M. Orchard et S. Newman, « The fundamental configuration and design of the compound helicopter », J. Aerosp. Eng., vol. 217, no 6, p. 297‑315, June 2003, DOI: 10.1243/095441003772538570.

[2] K. Ferguson et D. Thomson, « Flight dynamics investigation of compound helicopter configurations », J. Aircr., vol. 52, p. 156-167, Jan. 2015.

[3] M. Floros et W. Johnson, « Performance Analysis of the Slowed-Rotor Compound Helicopter», J. Am. Helicopter Soc., vol. 54, no 2, p. 22002, Apr. 2009, DOI: 10.4050/JAHS.54.022002.

[4] F. Frey et al., « Compound Helicopter X 3 in High-Speed Flight: Correlation of Simulation and Flight Test », Philadelphia, PA, May 2019, vol. 75th Annual Forum&Technology Display.

[5] P. Lorber et al., « Overview of S-97 RAIDER Scale Model Tests », presented at AHS International Forum 72, West Palm Beach, Florida, May 2016.

[6] O. Rand et V. Khromov, « Compound Helicopter: Insight and Optimization », J. Am. Helicopter Soc., vol. 60, Jan. 2015, DOI: 10.4050/JAHS.60.012001.

[7] C. M. Russell et W. Johnson, « Conceptual Design and Performance Analysis for a Large Civil Compound Helicopter », presented at AHS Future Vertical Lift Aircraft Design Conference, San Francisco, CA, Jan. 2012.

[8] T. C. A. Stokkermans, B. Soemarwoto, M. Voskuijl, R. Fukari, L. L. M. Veldhuis, et P. Eglin, « Aerodynamic installation effects of lateral rotors on a novel compound helicopter configuration », Phoenix, Az, may 2018, vol. 74, p. 12.

[9] J. Thiemeier, C. Öhrle, F. Frey, M. Keßler, et E. Krämer, « Aerodynamics and flight mechanics analysis of Airbus Helicopters' compound helicopter RACER in hover under crosswind conditions », CEAS Aeronaut. J., apr. 2019, doi: 10.1007/s13272-019-00392-3.

[10] H. Yeo et W. Johnson, « Aeromechanics Analysis of a Compound Helicopter », Phoenix, Az, May 2006, vol. 62nd Annual Forum, p. 16.

[11] Le Pape A., Gatard J., et Monnier J.-C., « Experimental Investigation of Rotor-Fuselage Aerodynamic Interactions », J. Am. Helicopter Soc., vol. 52, no 2, p. 99, Apr. 2007, DOI: 10.4050/JAHS.52.99.

[12] T. Renaud, M. Smith, M. Potsdam, et D. O'Brien, « Evaluation of isolated fuselage and rotor-fuselage interaction using Computational Fluid Dynamics », J. Am. Helicopter Soc., vol. 53, no 1, p. 3‑17, Jan. 2008, DOI: 10.4050/JAHS.53.3.

[13] L. Lefevre et V. Nowinski, « Characterization of the propeller for the experimental evaluation of the aerodynamic rotor/propeller interactions in hybrid compound helicopters », presented at ONERA - DLR Aerospace Symposium, Braunschweig, Germany, Nov 2020.

[14] R. Boisard, « Aerodynamic investigation of rotor/propeller interactions on a fast rotorcraft », Delft, The Netherlands, Sept. 2018, vol. 13, p. 14.